Nuclear Physics B137 (1978) 1–12

ELASTIC π^0 ELECTROPRODUCTION ABOVE THE RESONANCE REGION

Ch. BERGER, R. BÜHRING, G. DICK, R. GRIGULL,
H. MEYER-WACHSMUTH * and W. WAGNER
I. Physikalisches Institut der RWTH Aachen, Germany

H. ACKERMANN, T. AZEMOON, W. GABRIEL, H.D. MERTIENS,
H.D. REICH and G. SPECHT **
Deutsches Elektronen-Synchrotron DESY, Hamburg, Germany

E. GANSSAUGE
Universität Marburg, Germany

F. JANATA and D. SCHMIDT
Gesamthochschule Wuppertal, Germany

Received 8 December 1977
(Revised 13 February 1978)

We report on the measurement of the process $e + p \to e + p + \pi^0$ at energies above the resonance region. The pions are predominantly produced perpendicular to the electron scattering plane. The cross section shows a dip at the minimum momentum transfer. Both features are expected from comparison with photoproduction.

The differential cross section $d\sigma/dt$ for the photoproduction of single π^0 mesons above the resonance region ($\gamma + p \to \pi^0 + p$) shows a dip at $t = 0$ and at $t = -0.55$ GeV^2 [1,1a]. Experiments with linearly polarized photons have revealed dominance of $\sigma_\perp$ over $\sigma_\parallel$, where the symbols $\perp$ and $\parallel$ stand for production perpendicular and parallel to the polarization plane, respectively ‡. The dip structure and the dominance of $\sigma_\perp$ are both understood in terms of a (reggeized) ω exchange [3]. Since the electroproduction of π mesons can be interpreted as photoproduction by virtual photons ($q^2 < 0$), it is interesting to check if the properties discussed above extend to non-zero values of q^2.

* Now at Bertelsmann Verlag, Gütersloh, Germany.
** Now at Fachhochschule, Hamburg, Germany.
‡ A recent experiment in our energy range is described in ref. [2].

In the one-photon exchange approximation the electroproduction cross section can be written as

$$\frac{d^4\sigma}{dE'd\Omega_e dt\, d\phi} = \Gamma \frac{d^2\sigma_v}{dt\, d\phi}, \tag{1}$$

with

$$\frac{2\pi d^2\sigma_v}{dt\, d\phi} = \frac{d\sigma_U}{dt} + \frac{d\sigma_P}{dt}\epsilon\cos 2\phi + \epsilon\frac{d\sigma_L}{dt} + \sqrt{2\epsilon(\epsilon+1)}\frac{d\sigma_L}{dt}\cos\phi, \tag{2}$$

where

$$\Gamma = \frac{\alpha}{2\pi^2}\frac{E'}{E}\frac{M^2 - W^2}{2Mq^2}\frac{1}{1-\epsilon},$$

$$q^2 = -4EE'\sin^2\tfrac{1}{2}\theta_e,$$

$$\nu = E - E',$$

$$W^2 = q^2 + M^2 + 2\nu M,$$

$$\epsilon = [1 - 2(\nu^2 - q^2)\, q^{-2}\tan^2\tfrac{1}{2}\theta_e)]^{-1},$$

$$\frac{d\sigma_P}{dt} = \frac{1}{2}\left[\frac{d\sigma_\parallel}{dt} - \frac{d\sigma_\perp}{dt}\right],$$

$$\frac{d\sigma_U}{dt} = \frac{1}{2}\left[\frac{d\sigma_\parallel}{dt} + \frac{d\sigma_\perp}{dt}\right],$$

ϕ is the angle between the electron scattering plane and the reaction plane,

θ_e is the electron scattering angle,

t is the four-momentum transfer from the virtual photon to the pion.

The coordinate system used is described in detail in ref. [6].

The terms $d\sigma_U/dt$ and $d\sigma_P/dt$ are the only ones present in photoproduction with linearly polarized photons ($q^2 = 0$). For virtual photons ($q^2 < 0$) there are two additional terms $d\sigma_L/dt$ and $d\sigma_I/dt$, which describe production by longitudinally polarized photons and the transverse longitudinal interference, respectively. However, in electroproduction of neutral pions these terms are expected to be small due to the absence of Born terms and unnatural parity exchanges [4]. Brasse et al. [5] have published data on π^0 electroproduction at $\phi = 90°$. For this value of ϕ, σ_I does not contribute. Neglecting σ_L and *assuming* $\sigma_\parallel$ to be small as in photoproduction they

have compared the results of their experiment with photoproduction in a straightforward manner. It was very interesting to see that the dip at $t = -0.55$ GeV^2 already disappeared at the very small q^2 value of -0.22 GeV^2.

In this paper we report on an experiment carried out at DESY, at a primary electron energy of 4 GeV. The kinematical range covered is given by $-0.7 < q^2 < -0.1$ GeV^2, $1.8 < W < 2.7$ GeV, $t_{min} > t > -0.7$ GeV^2. The acceptance in ϕ was at maximum at $\phi = 0^\circ$ with the full ϕ cone available for $|t| < 0.15$ GeV^2.

The experimental layout is shown in fig. 1. The external electron beam was focussed onto a 4.5 cm liquid hydrogen target. Scattered electrons were detected by a spark chamber spectrometer. This spectrometer has been used in many experiments before and is described in ref. [6]. The neutral π mesons were detected *via* their two-γ decay in a large stack of 13 X 14 lead-glass shower counters 4.5 m away from the target. Each lead-glass module had a front size of 66 X 66 mm^2 and was 12.5 radiation lengths deep. The properties of this system are discussed in ref. [7]. The large magnet "Gilgamesch" was used as a cleaning magnet. Scintillation counters in front of the shower counter served for further suppression of charged background. A "two-γ trigger" was generated whenever more than 300 MeV was deposited in each of two separate cells. In the case of a two-γ electron coincidence all the information from the lead-glass stack was read out by an on-line computer and recorded on magnetic tape, whereas the spark chambers were photographed.

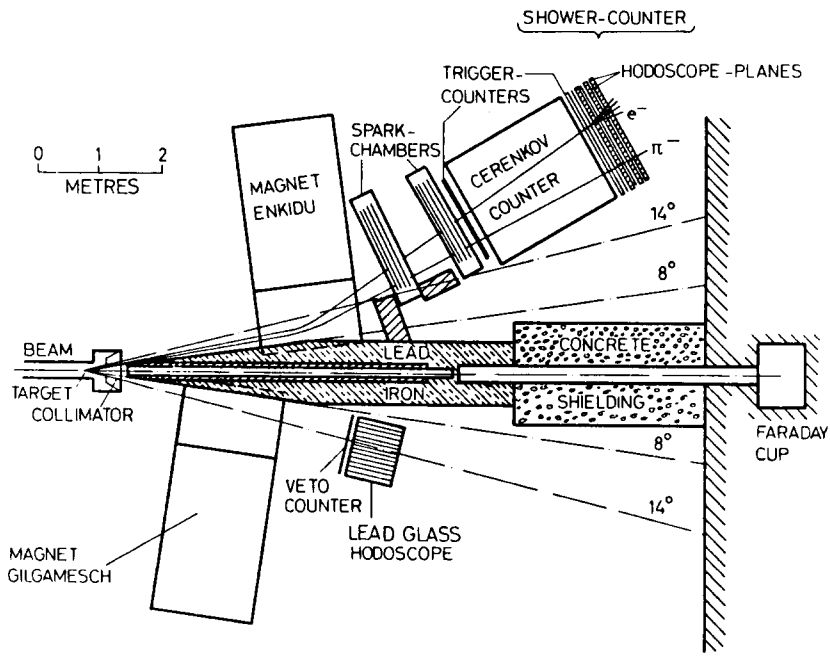

Fig. 1. Layout of the experimental set-up.

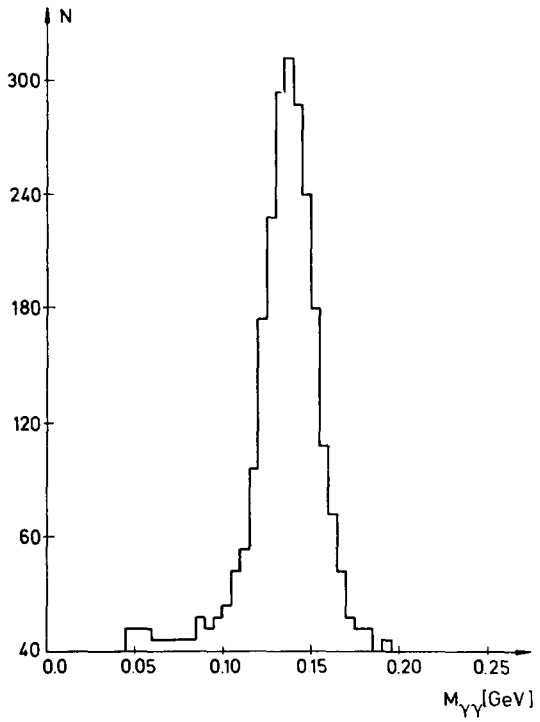

Fig. 2. Invariant-mass plot of the two-γ events.

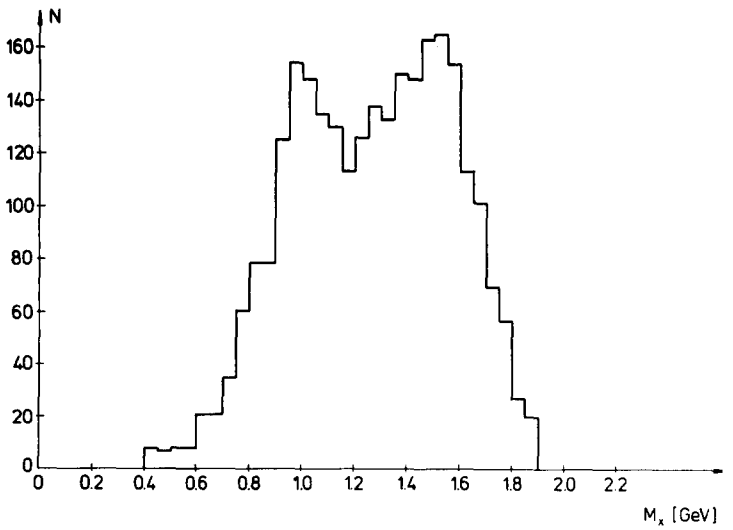

Fig. 3. Missing-mass distribution.

In fig. 2 a plot of the invariant mass $M_{\gamma\gamma}$ of the two detected γ-rays is shown, where a clear π^0 signal can be seen. The events where two adjacent cells were hit are not included as they imply a too-small opening angle in the π^0 decay and can only be produced by single γ-rays.

A plot of the missing mass M_X of the hadronic recoil system is shown in fig. 3. In order to separate the elastic events ($\gamma_v + p \rightarrow \pi^0 + p$) from inelastic channels we applied a cut in the opening angle 2α of the two γ-rays. Due to the π^0 decay kinematic most of the decay photons have an opening angle close to the minimum opening angle given by

$$\sin \alpha_{\min} = m_\pi / E_\pi \, .$$

For a given pion angle $\theta_{\pi\gamma_v}$ we can calculate E_π^{elastic} from the known momentum of the virtual photon. Inelastic channels have a lower energy leading to larger minimum opening angles and can therefore be rejected due to the good spatial resolution of the lead-glass stack.

In fig. 4 the remaining elastic peak is depicted, whose width is very well reproduced by Monte Carlo calculations, taking into account the spatial and energy resolution of the shower counter and the cut described above.

Cross sections have been corrected for events coming from the target walls (15% ± 1), accidentals (2% ± 1), conversion losses of the photons from π^0 decay (2% ± 0.5), the finite detection efficiencies of the electron arm (98% ± 0.2) and the branching ratio $\pi^0 \rightarrow 2\gamma$(98.83%). Radiative corrections were applied according to the method of Callan and Fuchs [8]. They never exceeded 12%.

In fig. 5 we display the distribution of the events in the W-q^2 plane, where the

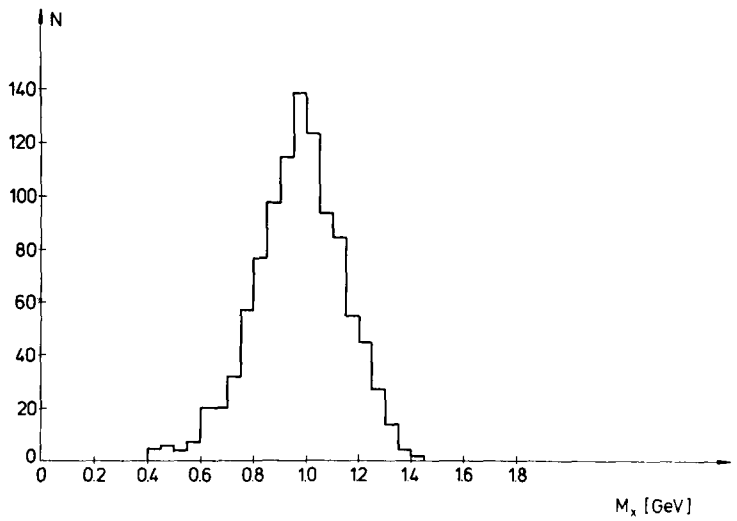

Fig. 4. Missing-mass distribution after cuts.

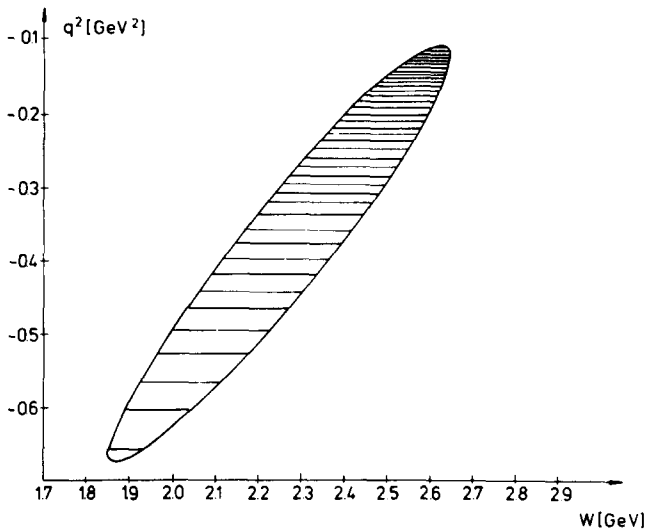

Fig. 5. Distribution of the events in the W-q^2 plane for an incoming electron energy of 4 GeV.

horizontal lines indicate the density of the data taken. For further analysis we divide all events in two groups: $W < 2.25$ GeV and $W > 2.25$ GeV, respectively.

In order to account for the variation of W and q^2 in these two data bins we weighted each event by a function $F(W^2, q^2)$ representing the well known energy dependence of the photoproduction cross section and the q^2 behaviour given by the ρ pole:

$$F(W^2, q^2) = \frac{1}{(W^2 - M_p^2)^{1.6}} \left(\frac{1}{1 - q^2/m_\rho^2} \right)^2 . \tag{4}$$

Typically, weighted and unweighted cross sections did not differ by more than 10%. For $W < 2.25$ GeV and $t > -0.15$ GeV^2 we have the full acceptance in ϕ, $0° < \phi < 360°$. The average q^2 and W values for all events are $q^2 = -0.5$ GeV^2, $W = 2.02$ GeV. In fig. 6 we plot $2\pi \mathrm{d}^2\sigma/(\mathrm{d}t\,\mathrm{d}\phi)$ *versus* ϕ for all events with $t_{\min} > t > -0.1$ GeV^2. From these data we have determined the various contributions to the cross section given in eq. (2). The solid line is the result of the fit, with the parameters given by

$$\frac{\mathrm{d}\sigma_U}{\mathrm{d}t} + \epsilon \frac{\mathrm{d}\sigma_L}{\mathrm{d}t} = 1.07 \pm 0.11 \ \mu\mathrm{b/GeV}^2 ,$$

$$\frac{\mathrm{d}\sigma_P}{\mathrm{d}t} = -0.61 \pm 0.12 \ \mu\mathrm{b/GeV}^2 ,$$

$$\frac{\mathrm{d}\sigma_I}{\mathrm{d}t} = -0.06 \pm 0.13 \ \mu\mathrm{b/GeV}^2 ,$$

with $\epsilon = 0.78$.

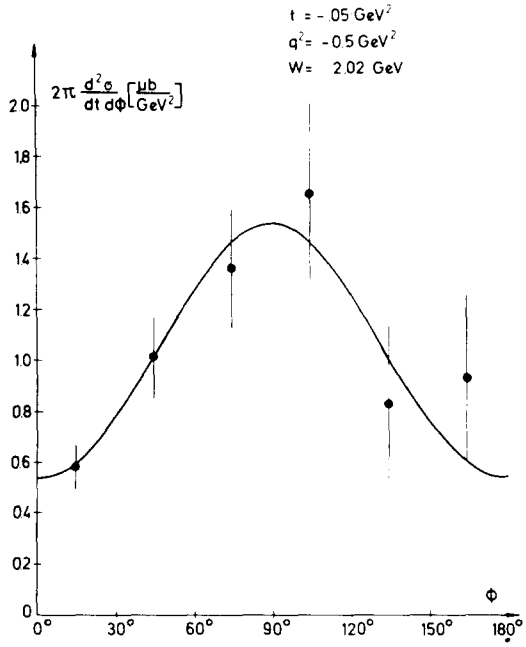

Fig. 6. $2\pi d^2\sigma/dt\,d\phi$ *versus* ϕ at $t = -0.05$ GeV^2, $-0.7 < q^2 < -0.03$ GeV^2, $1.8 < W < 2.25$ GeV.

Assuming that the same ϕ dependence as found above can be used in a slightly larger t range $t_{min} > t > -0.15$ GeV^2, we evaluated $d\sigma_U/dt + \epsilon\, d\sigma_L/dt$ as a function of t. The result is given in table 1 and fig. 7. In addition to our data we have plotted the cross sections of a recent photoproduction experiment [9] at almost the same value of W ($E_\gamma = 1.89$ GeV). We prefer to plot the data *versus* $t - t_{min}$ due to the t_{min} effect in electroproduction (t_{min} is typically -0.02 GeV^2). The $t - t_{min}$ depen-

Table 1
Cross sections $d\sigma_U/dt + \epsilon\, d\sigma_L/dt$ for $-0.7 < q^2 < -0.3$ GeV^2, $1.8 < W < 2.25$ GeV

t [GeV^2]	$\frac{d\sigma_U}{dt} + \epsilon \frac{d\sigma_L}{dt}$ [μb/GeV^2]
−0.020	0.76 ± 0.15
−0.035	0.82 ± 0.17
−0.05	1.05 ± 0.16
−0.07	1.30 ± 0.22
−0.09	1.63 ± 0.31
−0.11	1.91 ± 0.38
−0.14	1.88 ± 0.40

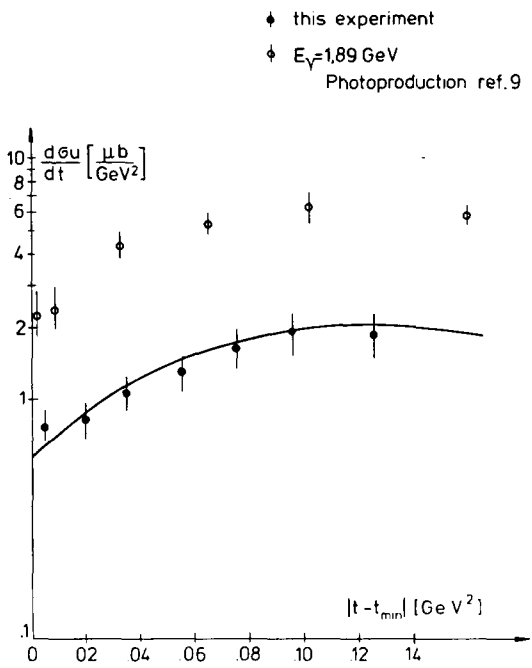

Fig. 7. $d\sigma_U/dt$ *versus* t for $t_{min} > t > -0.15$ GeV^2, $-0.7 < q^2 < -0.3$ GeV^2, $1.8 < W < 2.25$ GeV.

dence of both experiments is very similar, i.e. we have a clear forward dip. The solid line in fig. 7 was obtained by extrapolating the photoproduction data using the function $F(W^2, q^2)$ given in eq. (4). The result demonstrates that the q^2 behaviour is consistent with ρ dominance.

For $W > 2.25$ GeV we extend the t range up to $t = -0.7$ GeV^2. In fig. 8 and table 2 we give the cross section $2\pi d^2\sigma/dt\,d\phi$ for $\phi = 0°$ ($\Delta\phi = \pm 30°$). The average W and q^2 are given by $W = 2.48$ GeV and $q^2 = -0.275$ GeV^2. Also plotted in the figure are the results of the experiment of Brasse et al. [5] at $\phi = 90°$ (open circles). Because this experiment has been done at a slightly different value of W and q^2 the cross sections were again extrapolated using $F(W^2, q^2)$. The data indicate again a forward dip as seen in the small W range. In the region where both experiments overlap we see clear $\sigma_\perp$ dominance. Neglecting $d\sigma_I/dt$ we can use the two experiments to separate $d\sigma_P/dt$ and $d\sigma_U/dt + \epsilon\, d\sigma_L/dt$. The result is given in table 3.

If we assume $d\sigma_L/dt = 0$ we can calculate the asymmetry parameter A:

$$A = \frac{\sigma_\perp - \sigma_\parallel}{\sigma_\perp + \sigma_\parallel}.$$

The values for the parameter A are also included in table 3 and shown in fig. 9. We

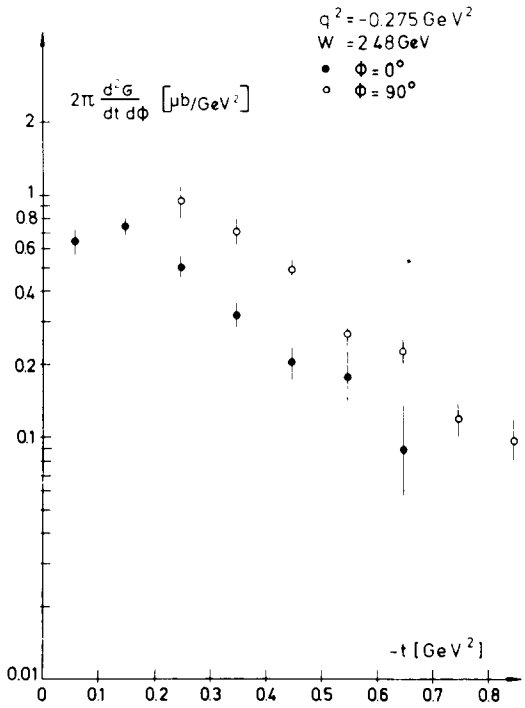

Fig. 8. $2\pi d^2\sigma/dt\,d\phi$ *versus* t for $-30° < \phi < 30°$, $t_{min} > t > -0.7$ GeV^2, $-0.45 < q^2 < 0$ GeV^2, $2.25 < W < 2.7$ GeV.

emphasize that the quoted errors are only due to the statistical errors of both experiments; normalization errors are not included. In order to investigate the influence of the normalization on the results we analysed our data in the t bin $0.15 < |t| < 0.35$ GeV^2 in the larger ϕ range $-50° < \phi < 50°$. The cross section $2\pi d^2\sigma/dt\,d\phi$ is

Table 2
Cross sections $2\pi d^2\sigma/dt\,d\phi$ for $-0.45 < q^2 < 0$ GeV^2, $2.25 < W < 2.7$ GeV, $-30° < \phi < +30°$

t [GeV^2]	$2\pi \frac{d^2\sigma}{dt\,d\phi}$ [nb/GeV^2]
−0.06	640 ± 79
−0.15	739 ± 52
−0.25	502 ± 40
−0.35	315 ± 33
−0.45	202 ± 32
−0.55	177 ± 39
−0.65	88 ± 44

Table 3
Cross sections and asymmetry parameters evaluated from ref. [5] and this experiment

t [GeV^2]	$\frac{d\sigma_P}{dt}$ [nb/GeV^2]	$d\sigma_U/dt + \epsilon\, d\sigma_L/dt$ [nb/GeV^2]	$A = \frac{\sigma_\perp - \sigma_\parallel}{\sigma_\perp + \sigma_\parallel}$
−0.25	−420 ± 131	705 ± 69	0.60 ± 0.15
−0.35	−373 ± 74	495 ± 39	0.75 ± 0.13
−0.45	−273 ± 57	333 ± 30	0.82 ± 0.16
−0.55	− 85 ± 46	218 ± 24	0.39 ± 0.24
−0.65	−129 ± 48	150 ± 25	0.86 ± 0.44

shown in fig. 10. A fit to the form

$$\frac{2\pi d^2\sigma}{dt\, d\phi} = \frac{d\sigma_U}{dt} + \epsilon \frac{d\sigma_L}{dt} + \epsilon \frac{d\sigma_P}{dt} \cos 2\phi$$

yields

$$\frac{d\sigma_U}{dt} + \epsilon \frac{d\sigma_L}{dt} = 840 \pm 90 \text{ nb/GeV}^2 ,$$

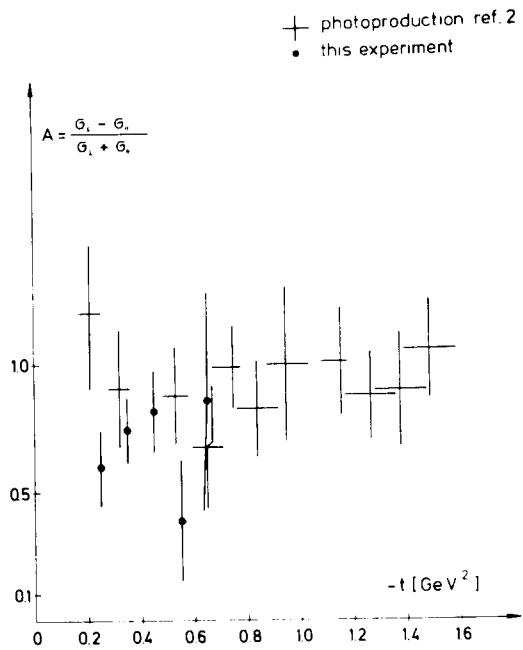

Fig. 9. Asymmetry parameter *versus* t.

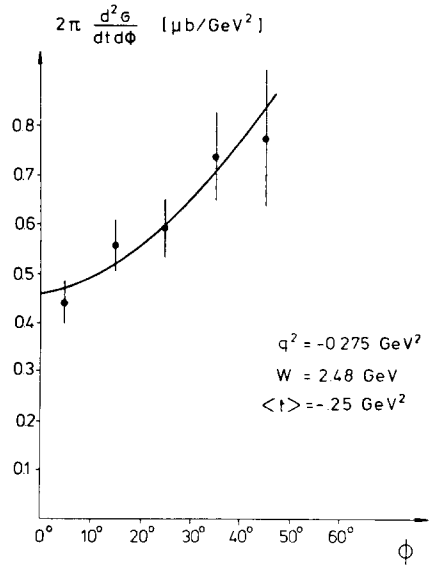

Fig. 10. $2\pi d^2\sigma/dt\,d\phi$ *versus* ϕ for $-0.1 < q^2 < -0.45$ GeV^2, $2.25 < W < 2.7$ GeV.

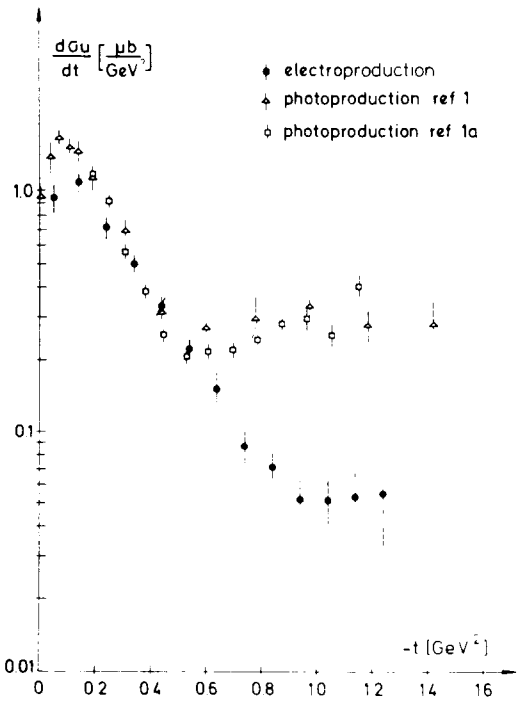

Fig. 11. Comparison of $d\sigma_U/dt$ with results from photoproduction.

$$\frac{d\sigma_P}{dt} = -740 \pm 110 \text{ nb/GeV}^2 ,$$

compatible with the results of table 3.

To compare the values of A obtained in electroproduction and photoproduction we have included the results of ref. [2] in fig. 9. The average asymmetry parameter A seems to be somewhat smaller than that in photoproduction. On the other hand, we clearly do not have $d\sigma_\parallel/dt = d\sigma_\perp/dt$, which is the behaviour preferred by quark model calculations [10].

Finally we can evaluate $d\sigma_U/dt$ in a large t-range combining the two experiments. In the region where both experiments overlap, the measured values of A were used. For $t > -0.25$ GeV^2 ($\phi = 0°$ data) and for $t < -0.65$ GeV^2 ($\phi = 90°$ data) we have assumed that A is constant in the whole t range and is given by the average measured value $A = 0.65$. These results are shown in fig. 11. The photoproduction data are taken from refs. [1,1a] and extrapolated according to eq. (4). The agreement for $|t| < 0.6$ GeV^2 is striking. In the light of these results the rapid disappearence of the dip at $t = -0.55$ GeV^2 is even more intriguing.

We thank the DESY Hallendienst and our technicians for their invaluable help during the course of the experiment. The Aachen and Wuppertal members of the collaboration are indebted to the DESY Directorium for their kind hospitality. The Aachen part of the group appreciates very much the constant encouragement of Prof. K. Lübelsmeyer.

References

[1] M. Braunschweig, W. Braunschweig, D. Husmann, K. Lübelsmeyer and D. Schmitz, Nucl. Phys. B20 (1970) 191.
[1a] W. Braunschweig, W. Erlewein, H. Frese, K. Lübelsmeyer, H. Meyer-Wachsmuth, D. Schmitz and A. Schultz von Dratzig, Nucl. Phys. B51 (1973) 167.
[2] P.J. Bussey, C. Raine, J.G. Rutherglen, P.S.L. Booth, L.J. Carroll, P.R. Daniel, C.J. Hardwick, J.R. Holt, J.N. Jackson, J.H. Norem, W.H. Range, F.H. Combley, W. Galbraith, V.H. Rajaratnam, C. Sutton, M.C. Thorne and P. Waller, Nucl. Phys. B104 (1976) 253.
[3] K. Lübelsmeyer, Proc. 4th Int. Symp. on electron and photon interactions at high energies, Liverpool, 1969, ed. D.W. Braben.
[4] H. Harari, Proc. 1971 Int. Symp. on electron and photon interactions at high energies, Cornell University, Ithaca, NY.
[5] F.W. Brasse, W. Fehrenbach, W. Flauger, J. Gayler, S.P. Goel, R. Haidan, U. Kötz, V. Korbel, D. Kreinick, J. Ludwig, J. May, M. Merkwitz, K.H. Mess, B. Schmüser and B.H. Wiik, Phys. Lett. 58B (1975) 467;
K.A. Mess, Thesis, DESY Interner Bericht F35-71/1.
[6] C. Driver, K. Heinloth, K. Höhne, G. Hofmann, P. Karow, D. Schmidt, G. Specht and J. Rathje, Nucl. Phys. B30 (1971) 245.
[7] Ch. Berger, R. Bühring, G. Dick, W. Erlewein, R. Grigull, N. Mistry and D. Trines, Nucl. Instr. 130 (1975) 507.
[8] G. de Callan and C. Fuchs, Nuovo Cim. 38 (1965) 1594.
[9] W. Brefeld, D. Husmann, W. Jansen, B. Löhr, K. Reichmann and H. Schilling, Nucl. Phys. B100 (1975) 93.
[10] O. Nachtmann, Nucl. Phys. B115 (1976) 61.